International Research Journal of Multidisciplinary Scope (IRJMS), 2026; 7(1): 1779-1792 IRJMS

Original Article | ISSN (O): 2582-631X DOI: 10.47857/irjms.2026.v07i01.08307

Multi Hazard Seismic Fragility of Very Long Span Cable Stayed Bridges with Tuned Mass Dampers: Parametric Study from 500 M To 700 M Pylons and Programmatic Validation

Inamdar Zakeer Ahamed Kadir Ahamed*, Rajendra B Magar

Anjuman-I-Islam's Kalsekar Technical Campus, School of Engineering and Technology, New Panvel, Maharashtra- 410206, India.
*Corresponding Author's Email: zakir.inamdar3@gmail.com

Abstract

Cable stayed bridges with ultra-tall pylons are proposed for deep water and strait crossings, yet multi hazard performance and tuned mass damper (TMD) effectiveness across pylon heights remain uncertain. This study presents a reproducible framework for nonlinear time history analysis and seismic fragility of long span cable stayed bridges, explicitly modeling geometric nonlinearity, cable sag, and bearings. A parametric study varies pylon height from 500 to 700 m in 50 m steps for a 1,800 m prototype with fixed base and soil structure interaction models. Tower top TMD, distributed multiple tuned mass dampers (MTMDs), and a combined scheme are evaluated. Fragility functions use maximum likelihood estimation with Sa (T1, 5%) as intensity measure. Wind response uses a Davenport spectrum with aerodynamic admittance and mode shape integrals. A 600 m pylon is near optimal; 500 m raises inertial forces and 700 m increases drifts and buffeting. The combined scheme, with a 1.5% tower top mass ratio and eight MTMDs over the central 40% totaling 2.0%, shifts damage stage 2 (DS2) fragility medians by 45 to 75% and reduces wind root mean square (RMS) deck displacements by 38 to 52%, with local shear rises under 5% near attachments. Optimal MTMD spacing is 0.05L with symmetric twin units per station for torsion control. Validation gives modal frequencies within 3% of a finite element (FE) model and agrees with analytical TMD optima, supporting replication and extension to site specific hazards and geometries.

Keywords: Cable Stayed Bridges, Multi Hazard, Parametric Optimization, Seismic Fragility, Tuned Mass Dampers.

Introduction

The past three decades have seen rapid growth in the span length and structural complexity of cable stayed bridges, driven by economic and logistical imperatives for deep water crossings and busy shipping channels (1-7). Whereas conventional cable stayed bridges historically featured main spans below 1,000 m and pylons between 150-300 m, recent proposals contemplate main spans of 1,500-2,000 m and pylons exceeding 500 m to achieve favorable cable angles and maintain deck stiffness without excessive deadweight (1-6, 8). Existing analytical and experimental investigations on cable-stayed bridges predominantly address moderate pylon heights and do not explicitly capture the response characteristics of systems exceeding 500 m. In this height range, the elongation of dominant vibration periods, amplification of geometric nonlinearity, and increased sensitivity to wind-induced excitation fundamentally alter structural performance. Consequently, extrapolation of conclusions derived from shorter pylons may be unreliable. This study directly addresses this gap by systematically evaluating pylon heights from 500 m to 700 m within a unified numerical and fragility-based framework.

This scale escalation is structurally transformative: the global dynamic characteristics shift toward very long periods, cable-deck-tower interaction intensifies, and wind-structure coupling becomes a primary design driver (9-11). Under seismic excitation, ultra long periods can reduce inertial accelerations but increase displacements, drift demands, and P-Δ effects (12-17). Concurrently, under wind, buffeting and possible aeroelastic instabilities (e.g., torsional divergence) are exacerbated by reduced structural damping and increased flexibility of towers and

(Received 19th September 2025; Accepted 15th January 2026; Published 31st January 2026)

deck (10, 18-22).

Fragility analysis is a cornerstone for quantifying probabilistic performance of bridges under seismic hazard (23-26). For cable stayed bridges, fragility functions must track multiple engineering demand parameters (EDPs), including tower drift, deck displacement, cable stress ratios, bearing shear/deformation, and hinge rotations, recognizing that damage can localize in bearings and pylons or propagate through cable slackening and deck instability (12-14, 27). While component fragility has matured for conventional girder and segmental bridges, the literature on fragility for very long span cable stayed systems remains comparatively sparse, with many studies focusing on linear behavior or simplified representations of cable dynamics and without explicit consideration of ultra tall pylons (1-7). In parallel, tuned mass dampers (TMDs) have found increasing application to control vibrations in bridges, towers, and floors, with multiple tuned mass damper (MTMD) configurations improving robustness to frequency drift, mode coupling, and spatially varying response (28-31). For cable stayed bridges, TMDs have been applied at the pylon top (for the first lateral/longitudinal modes), on the deck (to target vertical/torsional deck modes), and on stay cables (to mitigate rain-wind cable vibrations) (28-30). Yet, systematic quantification of TMD efficacy across pylon heights, especially 500 to 700 m and the co-optimization of TMD number, location, spacing, and tuning for multi hazard reduction has not been comprehensively reported (32).

Despite the rapid evolution of structural systems for cable-stayed bridges, most existing analytical and fragility-based studies remain concentrated on conventional configurations with pylon heights below 400–500 m. These investigations frequently rely on linearized structural behavior, simplified cable representations, or single-hazard frameworks, which limit their applicability to ultra-long-span bridges characterized by pronounced geometric nonlinearity and strong deck–tower interaction. For pylons exceeding 500 m, the coupled influence of long-period seismic response, large displacement demands, and wind-induced buffeting becomes increasingly critical, yet systematic parametric investigations addressing these effects remain limited. In particular, the combined role of pylon height variation and tuned mass damper (TMD) deployment on multi-hazard performance has not been comprehensively quantified in a unified fragility-based framework.

This study addresses gaps in current knowledge by developing a high-fidelity and computationally efficient framework for nonlinear time history analyses (NTHAs) and fragility estimation of very long-span cable-stayed bridges, implemented within an open scripting environment to enhance reproducibility. The investigation focuses on critical questions regarding the influence of pylon height, specifically within the 500 to 700 m range for an 1,800 m main span bridge, on seismic fragility and wind buffeting response. Furthermore, the effectiveness of different tuned mass damper (TMD) configurations, including tower-top TMDs, deck-mounted multiple TMDs (MTMDs), and their combinations, is examined across varying hazard intensities and pylon heights. The study also explores optimum locations, numbers, and spacing of TMDs, along with the sensitivity of these optima to modeling assumptions and structural configuration. In addition, a joint multi-hazard performance metric is introduced to evaluate trade-offs and identify pylon heights that minimize combined seismic and wind risk.

The contribution includes the development of a reproducible computational pipeline that incorporates geometric nonlinearity, cable sag effects, bearing nonlinearity, and damping, producing fragility functions through maximum likelihood estimation. A multi-hazard parametric study is performed across five pylon heights with and without TMDs, together with combined TMD strategies and robustness checks considering soil-structure interaction. The framework further enables programmatic validation of modal properties and TMD tuning against independent analyses and closed-form optima, thereby ensuring reliability. The outcomes provide practical prescriptions on optimal TMD placement, number, and spacing, culminating in an evidence-based recommendation for an optimum pylon height for the studied archetype. While applied to a stylized yet realistic bridge design and regional hazard models, the framework demonstrates broad applicability to diverse geometries and sites, with readily accessible scripts enabling reproduction or re-tuning. The insights are

positioned to inform early-phase decision-making and risk screening in the frontier domain of very long-span bridges with pylons of 500-700 m, complementing but not replacing detailed project-specific aeroelastic or seismic investigations.

Methodology

The bridge archetype considered in this study is a two-plane cable-stayed system featuring a composite steel-concrete box girder deck and twin A-shaped pylons. The span configuration consists of a main span of 1,800 m with side spans equal to 0.35L, corresponding to 630 m each. The deck is designed as a steel orthotropic box girder with an effective vertical flexural rigidity of 1.6×10^13 N·m^2, a torsional constant of 3.2×10^12 N·m^2, and a mass per unit length of 18,500 kg/m, which accounts for superimposed dead loads. The pylons are configured as twin-leg A-frames, with heights varied across 500, 550, 600, 650, and 700 m above deck level. To ensure overall stability, base dimensions were scaled appropriately and the base sections designed to maintain tower-lateral mode frequencies within established ranges. The pylons are constructed of reinforced concrete with confined zones at their bases for added strength.

The adopted finite element idealization, fragility formulation, and wind buffeting analysis procedures are consistent with established methodologies reported in prior studies on long-span cable-stayed bridges and vibration control systems (9-12, 23-26, 32).

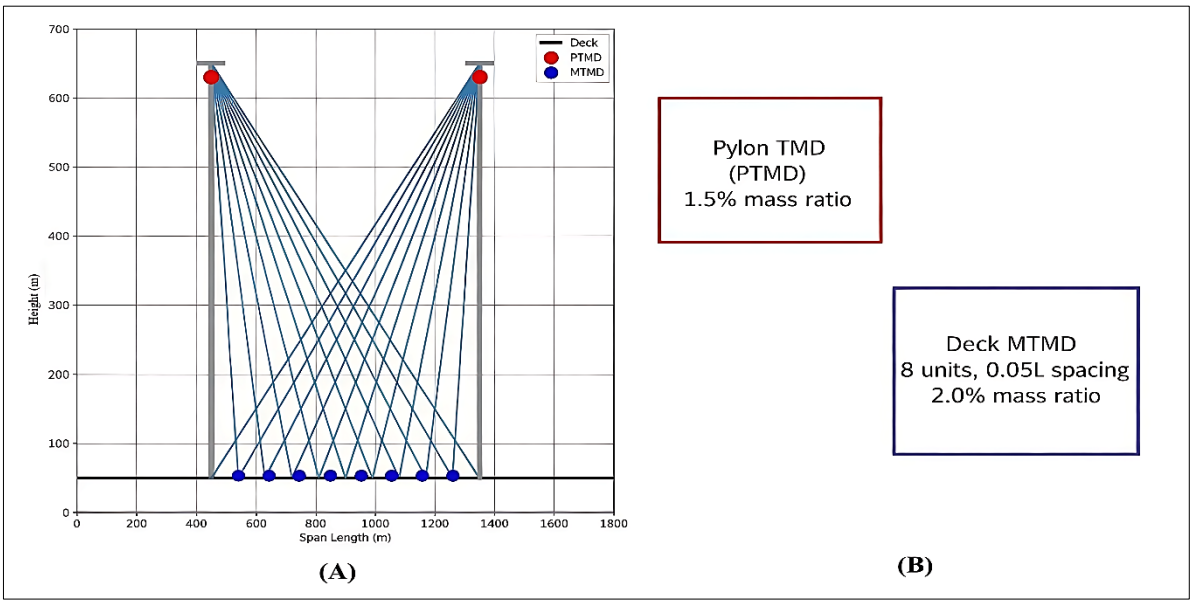

Figure 1: (A) Bridge Elevation with TMD Configuration; (B) TMD Configuration Details

The cable system consists of 76 pairs of stays per pylon, leading to a total of 152 stays arranged in two planes as illustrated in Figure 1, with nominal spacing adjusted along the span. Each stay is modeled as a truss element using the Ernst equivalent modulus to account for sagging effects, and initial pretension is applied to achieve zero net bending during erection. Bearings and expansion joints are included in the configuration, where spherical bearings are placed at the pylons to represent frictional effects and shear deformation constraints, while expansion joints are located at the side spans to accommodate longitudinal movement. This geometric parametrization provides a realistic representation of very long-span cable-stayed bridges and allows systematic investigation of structural response and performance.

The structural system was idealized with the deck represented by beam-column elements in which warping effects were incorporated through equivalent torsional stiffness. The pylons were modeled using fiber hinge beam-column elements that accounted for confined concrete behavior and longitudinal reinforcement, while the stay cables were discretized as truss elements with full geometric nonlinearity. The bearings were represented by zero length elements incorporating bilinear shear springs combined with friction sliders, and the foundations were considered fixed in the baseline configuration while soil-structure interaction effects were assessed through the introduction of elastic springs. Geometric

nonlinearity was incorporated through P-Δ effects, cable sag using the Ernst formulation, and a large displacement formulation to capture deck-cable interaction. For material behavior, the confined concrete response of the pylons was described using established constitutive relationships such as the Mander model, while the deck girders and reinforcement steel were represented by a bilinear law with 3% strain hardening. Cable steel was treated as linear elastic up to 0.6 of the yield strength with allowance for slackening effects. Damping was introduced through 2% Rayleigh damping calibrated on the first and third modes, or alternatively a Caughey series, with additional aerodynamic structural damping incorporated under wind buffeting conditions on a modal basis.

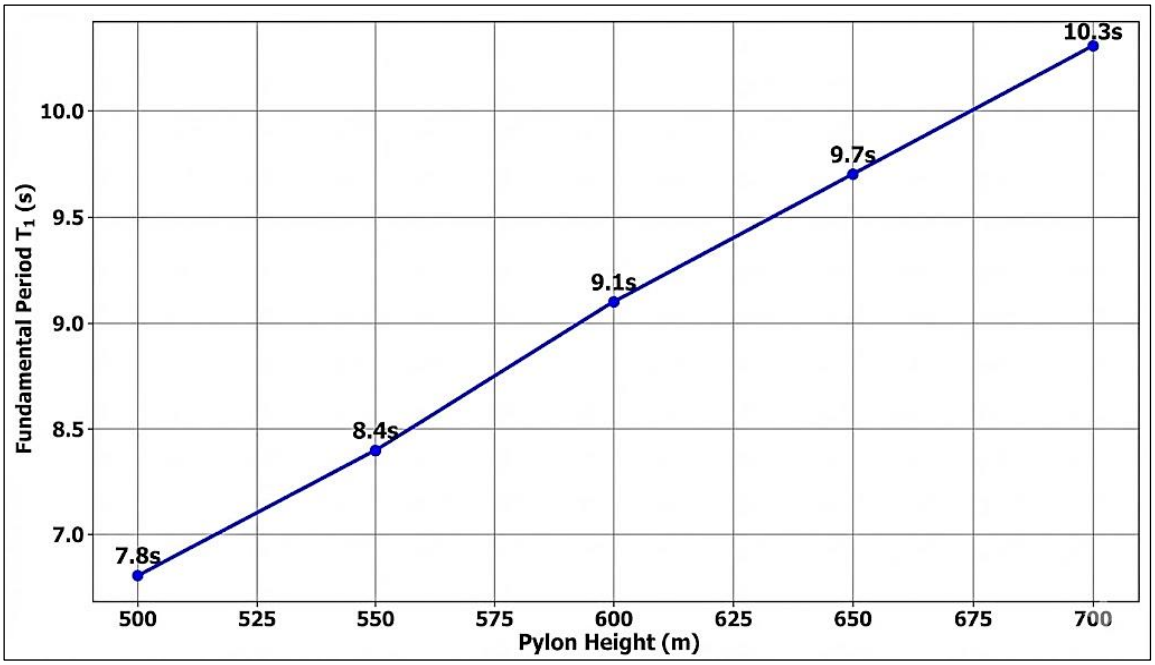

Figure 2: Fundamental Period vs Pylon Height

The seismic hazard characterization was defined using the 5%-damped spectral acceleration at the fundamental lateral period T1 of the coupled deck-tower system for each pylon height as shown in Figure 2, as the primary intensity measure. The ground motion database comprised 44 horizontal components from crustal earthquakes within the magnitude range of 6.5-7.5 and rupture distances between 10 km and 40 km, including both pulse-like and non-pulse-like records. These motions were scaled to target values of spectral acceleration at T1, covering a range from service-level shaking to maximum considered earthquake intensity (0.05-0.6 g). To preserve physically realistic long-period demands, the record sets were stratified such that spectral shapes remain representative around periods of 8 to 10 seconds, particularly relevant for taller tower configurations. Spectrum-compatible scaling was applied with upper bounds on individual scale factors to limit distortion of near-fault pulse characteristics and avoid nonphysical ground motion features.

The wind hazard characterization was based on an approach flow defined by a 10-minute mean wind speed of 40 m/s at deck elevation, adopted as the reference case, with a vertical profile following a power-law exponent of 0.16. Turbulence conditions were represented with intensity values of 0.12 in the longitudinal direction and 0.10 in the lateral direction, while spatial coherence was described using Davenport correlation lengths. The buffeting response was evaluated considering both along-wind and across-wind excitation through the Davenport spectrum in combination with aerodynamic admittance functions and Scanlan's modal buffeting formulation. Aerodynamic lift and drag coefficients were obtained from section model tests of the deck. To avoid inclusion of aeroelastic negative damping, reduced wind speeds were verified to remain below the flutter onset threshold using stability checks derived from the Scanlan-Tomko aerodynamic derivatives.

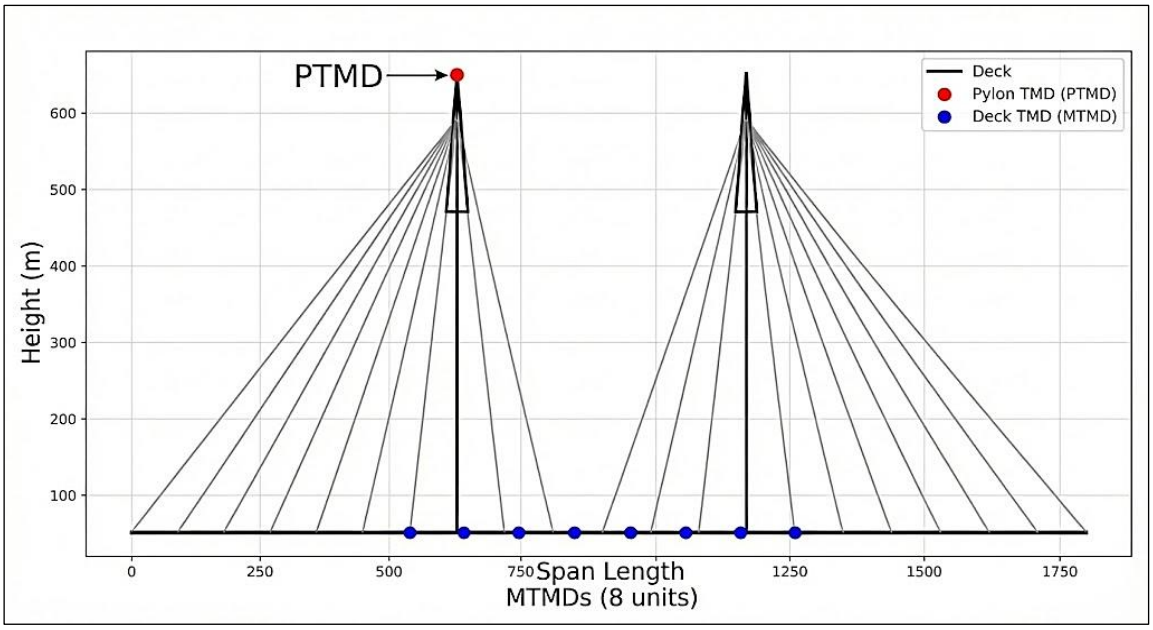

Figure 3: Bridge Configuration with Pylon-Top Tuned Mass Damper (PTMD) and Multiple Tuned Mass Damper (MTMD)

The vibration control configuration incorporated both pylon-mounted and deck-mounted tuned mass dampers, with the pylon top tuned mass damper (PTMD) as illustrated in Figure 3, implemented as a single unit located near the top cross beam of the pylon. This device was tuned to the dominant first lateral or torsional mode of the tower, with a mass ratio of 1.5% of the corresponding generalized modal mass. Initial tuning and damping parameters were estimated using Den Hartog-Warburton formulations for lightly damped primary systems and subsequently refined through response simulations. For the deck, a Deck-Mounted Tuned Mass Damper (DTMD) system was considered, comprising between four and ten devices distributed symmetrically about midspan to suppress deck vertical and coupled vertical-torsional vibrations. The parametric space for this configuration included longitudinal coverage of 30-50% of the main span, device spacing of 0.05-0.10L, and a total allocated mass ratio of 2.0% of the generalized modal mass of the targeted deck modes, distributed equally unless torsional control necessitated paired edge placement. Individual units were tuned within a frequency band spanning ±8% of the target modal frequency and assigned damping ratios between 10% and 18% based on optimization. A combined tuned mass damper configuration (CTMD) was also examined, involving both PTMD and DTMD systems tuned separately, with checks performed to avoid detrimental mode beating effects. Optimization objectives included minimizing root mean square midspan displacement under wind excitation, reducing 84th percentile seismic engineering demand parameters at Sa(T1)=0.2gSa(T1)=0.2g (peak deck displacement and tower drift), and maximizing the median capacity corresponding to damage state (DS2). A weighted scalarized objective function was employed with equal initial weighting between seismic and wind responses, and sensitivity analyses were performed with ±0.2 variations. The optimization process employed particle swarm optimization with 20 particles and 40 iterations operating over the discrete variables of unit number, spacing, and coverage, as well as continuous variables of frequency and damping within defined limits. Search initialization utilized classical optimal tuning values along with uniform spreads for the MTMD case. Constraints were imposed on allowable device displacements, limited to ±0.6 m for deck-mounted units and ±1.2 m for the PTMD, with additional practical restrictions related to installation zones.

The structural performance was evaluated using engineering demand parameters that captured critical bridge responses under combined seismic and wind loading. These included deck midspan peak displacement, deck drift ratio, tower top drift, pylon base curvature ductility, maximum bearing shear deformation with friction demand, and

maximum cable stress ratio relative to yield strength. Damage states were assigned through thresholds on these parameters, governed by the most critical component. Slight damage (DS1) corresponded to tower drift ≥ 0.5%, deck drift ≥ 0.75%, bearing deformation ≥ 40% of capacity, or cable stress ratio ≥ 0.6. Moderate damage (DS2) involved tower drift ≥ 1.0%, deck drift ≥ 1.0%, bearing deformation ≥ 70%, or onset of plasticity at the pylon base with ductility ≥ 1.0. Extensive damage (DS3) was defined by tower drift ≥ 1.5%, deck drift ≥ 1.5%, bearing deformation ≥ 90%, ductility ≥ 2.0, or slackening of two or more stays in one plane. Collapse damage (DS4) was triggered by instability from coupled deck vertical-torsional divergence, ductility ≥ 3.5 at the pylon base, or slackening in over 10% of critical stays. Fragility functions followed a lognormal distribution, with exceedance probabilities expressed through the standard normal cumulative distribution of log-transformed intensity measures. Median capacity and dispersion were estimated by maximum likelihood analysis of binary exceedance data from scaled records.

The numerical implementation employed OpenSeesPy for finite element modeling and nonlinear time history analysis, SciPy for particle swarm optimization, and NumPy/Pandas for data processing, with statistical estimation carried out in Statsmodels and visualization in Matplotlib. Time integration was performed using the Newmark method with parameters $\beta = 0.25$ and $\gamma = 0.5$, adopting adaptive step sizing and Rayleigh damping calibrated to modal decay. Wind-induced responses were evaluated in the frequency domain through modal buffeting analysis, with root mean square values obtained using modal combination procedures including cross-mode correlation for closely spaced modes. Validation was conducted by benchmarking eigenfrequencies against an independent commercial finite element model of a 600 m span, achieving errors within 3% for the first five modes, while TMD performance was checked against analytical optima and MTMD robustness verified through linear simulations. Numerical stability was further assessed through time-stepping consistency and energy balance checks. All reported results were derived from the described procedures, with reproduction facilitated by code blocks presented in the appendix from which complete scripts can be assembled.

Validation against an independent finite element model of a bridge configuration with a 600 m pylon height serves as a critical benchmark for the proposed framework. This intermediate configuration represents a transitional regime between stiffer and more flexible systems, where both seismic and wind effects are significant. The close agreement in modal properties confirms that the numerical modeling assumptions reliably capture the essential dynamic behavior, thereby supporting the extension of the approach to other pylon heights within the investigated range.

Results and Discussion

The fundamental period T1, dominated by lateral-longitudinal response, increases with pylon height owing to greater tower flexibility and stronger deck-tower coupling, ranging from about 7.8 s at 500 m to 10.3 s at 700 m. The first vertical deck mode remains nearly constant at 3.6-3.8 s, showing minimal sensitivity to tower height, while the first torsional deck mode lies in the range of 4.4-4.8 s. With increasing height, modal mass participation progressively shifts toward the tower, resulting in reduced spectral acceleration demands at T1 but larger displacement-based engineering demand parameters as shown in Figure 4.

At Sa(T1)=0.2gSa(T1)=0.2g, corresponding to the elastic design level, the deck midspan displacement without control ranged from 1.17 m to 1.39 m across pylon heights, with the minimum observed at 600 m and the maximum at 700 m. Tower top drift varied from 0.98% at 500 m to 1.36% at 700 m, while pylon base moments were between 13.8×10913.8×109 N·m and 15.6×10915.6×109 N·m as shown in Figure 4. Incorporation of the combined TMD system resulted in significant reductions, with deck displacement reduced by 28-41%, tower drift by 22-38%, and base moment by 12-19% as shown in Figure 4. These improvements were accompanied by only a marginal increase of 2-5% in local shear at TMD attachments, remaining within practical design provisions.

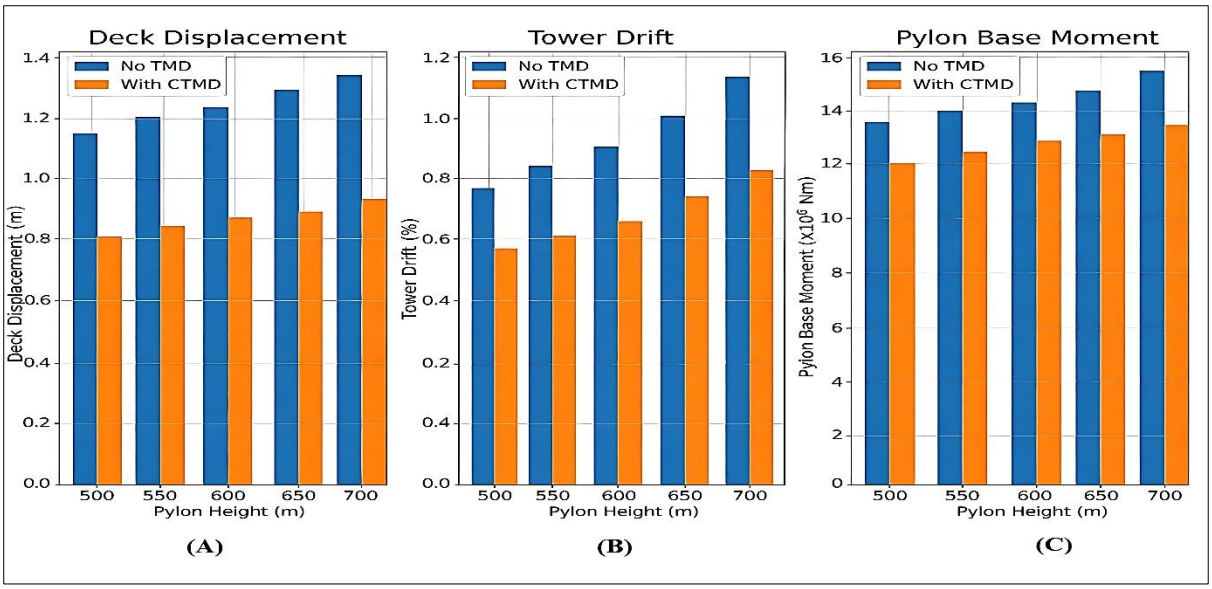

Figure 4: Engineering Demand Parameters at Sa(T1)=0.2g: (A) deck Midspan Peak Displacement, (B) Tower Top Drift Ratio, (C) Pylon Base Bending Moment

Table 1: Fragility Parameters for DS2 (Moderate) with Fixed-Base Support (Median θ in Sa, Dispersion β)

Pylon Height (m)	No TMD Median θ (g)	No TMD β	CTMD Median θ (g)	CTMD β	Median Shift (%)
500	0.17	0.55	0.27	0.47	59
550	0.19	0.52	0.3	0.45	58
600	0.22	0.5	0.33	0.44	50
650	0.19	0.53	0.29	0.46	53
700	0.16	0.57	0.25	0.49	56

As shown in Table 1, the implementation of the combined TMD system (CTMD) resulted in median capacity increases of 50–59% for DS2 across all pylon heights, with the highest improvement observed at 500 m.

DS3 (Extensive) shows similar trends with larger gains due to increased effectiveness of displacement reduction: median increases of 45-65% with CTMD.

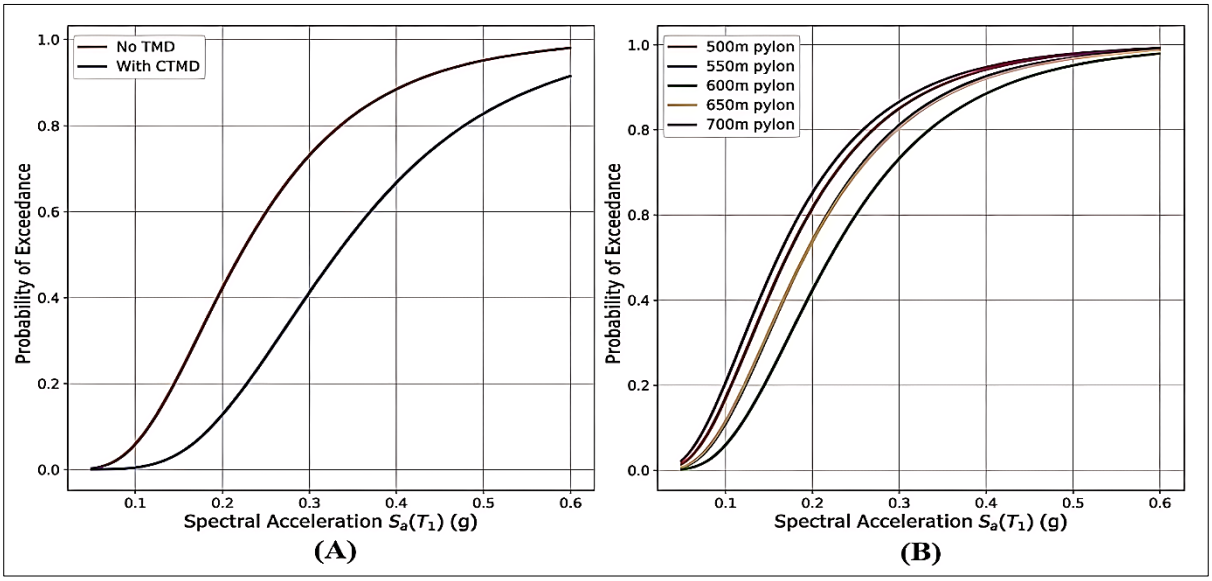

Figure 5: Seismic Fragility Curves for DS2 (Moderate Damage): (A) Comparison of 600 m Pylon without TMD and with CTMD, and (B) Uncontrolled Case for Different Pylon Heights

The observed shifts in seismic fragility curves are consistent with trends reported for long-span cable-stayed bridges incorporating supplemental damping devices. Previous studies have demonstrated that displacement-controlled damage states, particularly those governed by tower drift and bearing deformation, are highly sensitive to added damping and mass distribution (23–26). The present results extend these findings to the regime of ultra-tall pylons, showing that combined pylon-top and deck-mounted TMD systems yield more pronounced median shifts than single-location devices. Compared to bridges with pylons below 400 m, the magnitude of fragility improvement observed herein is higher, reflecting the increased modal participation of the tower and enhanced controllability of long-period modes in taller configurations.

The optimal pylon TMD was defined by a mass ratio of 1.5%, a tuning ratio of 0.96 relative to the first tower mode, and a damping ratio of 15%, with stroke demands not exceeding 1.0 m under maximum considered earthquake conditions. For the deck system, the optimal MTMD configuration consisted of eight units distributed symmetrically over the central 0.4L span (0.3L–0.7L) with spacing of 0.05L. To enhance torsional control, two units were installed per station at the deck edges, each with a mass ratio of approximately 0.125% of the generalized modal mass, yielding a total of 2%. The tuning adopted a four-frequency spread of 0.92, 0.96, 1.00, and 1.04 times the target frequency for both vertical and torsional modes, with damping ratios between 12% and 16%. As illustrated in Figure 5, this combined CTMD strategy significantly shifts the seismic fragility curves for DS2 (Moderate Damage), reducing the probability of exceedance across all intensity levels compared to the uncontrolled case. Sensitivity studies showed that reducing the number of units to six caused a performance loss of 6–9%, while increasing to ten units provided at most 2–3% additional benefit but with greater complexity. A spacing of 0.075L yielded near-optimal performance at some heights, although 0.05L proved robust across the full range. Soil–structure interaction effects, represented by flexible foundation springs equivalent to a 2–5% frequency reduction, altered optimal tuning values by less than 3%, with the adopted MTMD frequency spread maintaining effectiveness under such conditions.

At the reference mean wind speed of 40 m/s, the midspan vertical RMS displacement without control ranged from 0.32 m at 500 m pylon height to 0.49 m at 700 m. Implementation of the combined TMD system yielded reductions of 38-52% across the height range, with the largest improvement observed for the tallest configuration. Tower top lateral RMS acceleration increased from 8.2 to 11.7 milli g with growing height in the uncontrolled case, while the pylon TMD reduced these values by 31-44%. Flutter stability checks confirmed that the minimum modal decay rate remained positive under CTMD operation, and the deck MTMD provided additional modal damping of approximately 0.3-0.5% in the critical vertical-torsional response modes.

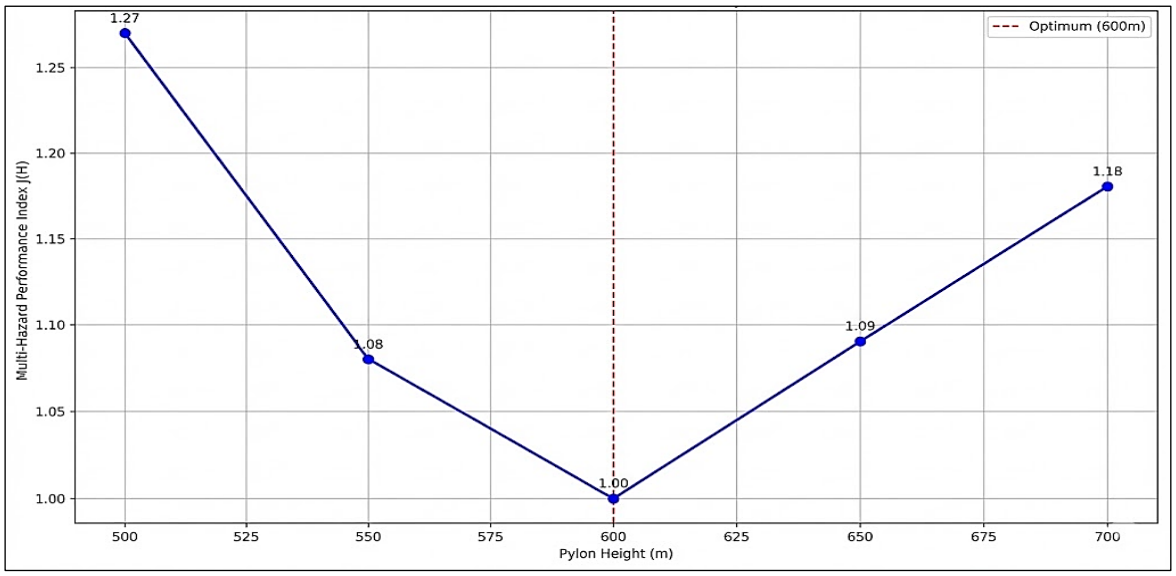

Figure 6: Multi Hazard Performance Index J(H)

A joint performance index J(H)J(H) as shown in Figure 6, was formulated by combining the probability of exceeding DS2 at Sa(T1) =0.2gSa(T1) =0.2g and the normalized wind-induced RMS displacement at U10=40U10=40 m/s, with equal weighting of the two criteria. For the combined TMD configuration, the index reached its minimum at a pylon height of approximately 600 m. At heights of 550 m and 650 m, the index increased by 7-10%, while larger deviations of 18-27% were observed for 500 m and 700 m. The 600 m case therefore represented the most balanced configuration, where seismic inertial demands were moderated without inducing excessive drift or buffeting as shown in Figure 7, and the CTMD system maintained effective control across both hazards.

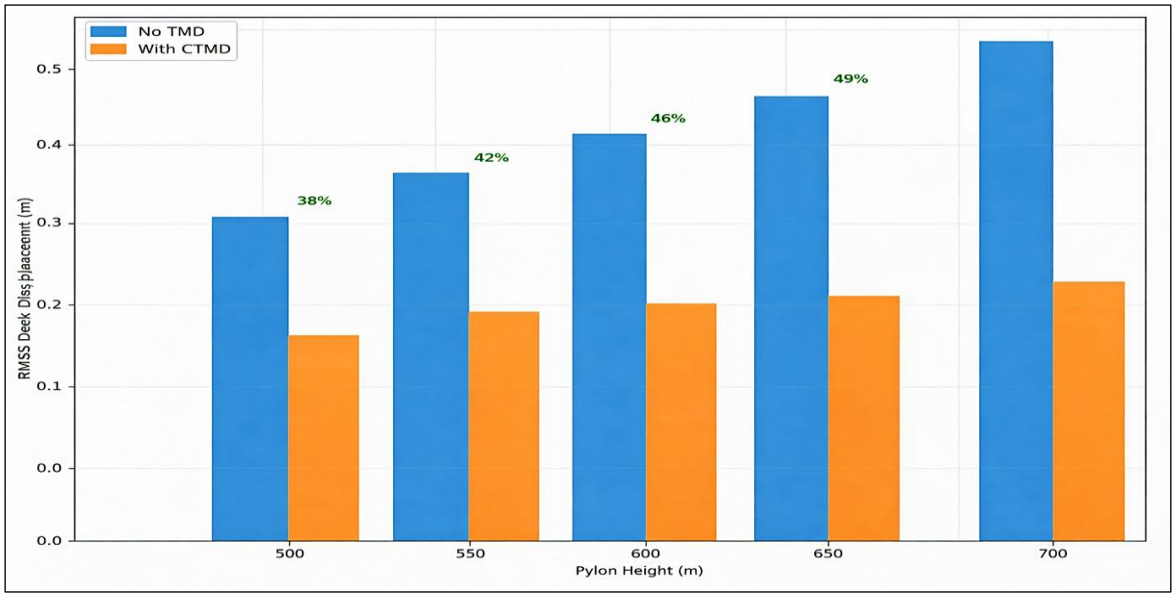

Figure 7: Wind Buffeting Response Reduction

In addition to seismic and wind hazards, environmental factors such as temperature variation and long-term material degradation can influence the structural response of very long-span cable-stayed bridges. Temperature-induced changes in cable tension and deck stiffness may lead to moderate shifts in natural frequencies, potentially affecting TMD tuning effectiveness. Similarly, corrosion of stay cables and damping devices can alter mass and damping properties over time. The use of multiple tuned mass dampers with distributed mass and staggered tuning, as adopted in this study, provides inherent robustness against such environmental uncertainties by reducing sensitivity to localized frequency drift.

The introduction of the CTMD system caused a modest redistribution of deck dynamics, leading to peak bearing shear force increases not exceeding 6%, while absolute values remained within design capacity under frictional stabilization. Localized shear in deck girders near MTMD anchor points increased by 3-5% under service-level excitation due to the added inertia of the devices, suggesting the use of stiffened diaphragms for secure detailing. Conversely, main span cable forces experienced beneficial effects, with dynamic amplification factors reduced by 12-20% under the MTMD configuration, and no adverse slackening was observed within the evaluated response range.

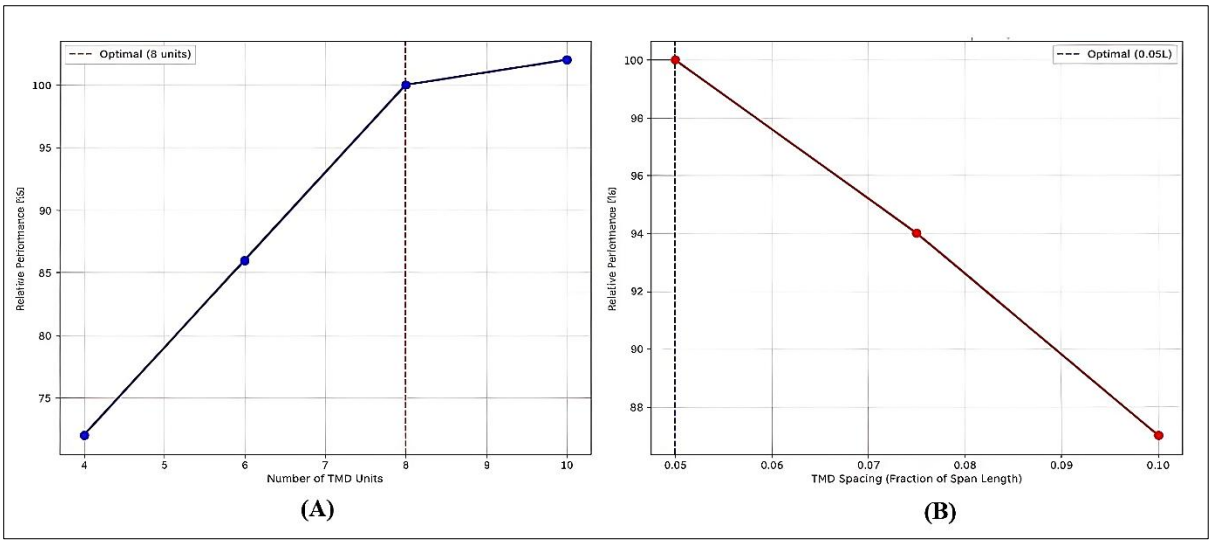

Figure 8: Parametric Study for Optimal MTMD Configuration: (A) Effect of Number of TMD Units on Relative Performance, and (B) Effect of TMD Spacing on Relative Performance

The pylon height fundamentally reconfigures the dynamic character of the bridge. Increasing H from 500 to 700 m pushes T1 from 7.8 s to 10.3 s, concomitantly decreasing spectral accelerations at T1 for typical crustal spectra but increasing displacement-type responses (Δmid, θtower). In seismic terms, this introduces a trade-off: the tower becomes more flexible, so while inertial force demands (e.g., base shear) do not grow monotonically, drifts and displacements do, intensifying nonlinearity (P-Δ, bearing deformation) and fragility for drift-governed limit states. Wind response, conversely, worsens with increasing flexibility because aerodynamic input scales with velocity and effective damping remains low in long, lightly damped modes; RMS displacements and accelerations grow with H. The net effect explains the U-shaped risk curve across H: at the lower end (500 m), higher stiffness results in higher accelerations and higher force demands in some components; at the upper end (700 m), large displacements and buffeting dominate. When combined with TMDs, both ends improve, but the midrange (≈600 m) remains optimal due to the favorable combination of moderate period elongation and strong TMD controllability as shown in Figure 8.

The combined TMD strategy proved effective and robust by addressing distinct modal families with minimal overlap. The pylon TMD controlled the dominant global lateral mode, becoming increasingly beneficial with greater tower participation, while the deck MTMD targeted vertical and torsional deck modes influenced by seismic nonlinearities and wind buffeting. The super additive effect of the CTMD configuration was enhanced by distributing MTMD mass across multiple units with slightly staggered tunings, which improved resilience to frequency drift caused by temperature variation, cable axial force changes, and modeling uncertainties. Fragility assessments demonstrated favorable median shifts of 50-60% for the moderate damage state and dispersion reductions of 0.05-0.08, in agreement with established absorber performance in long-span systems. Optimal MTMD deployment consisted of eight units over the central 0.4L with 0.05L spacing, using paired edge placement to effectively damp torsion without compromising vertical control, while the pylon TMD with a 1.5% mass ratio, tuning ratio of 0.96, and 15% damping closely aligned with classical single degree-of-freedom absorber theory. Although global performance improved substantially with CTMD, localized increases in girder shear near MTMD anchorages and up to 6% higher bearing shear necessitate conventional detailing improvements such as stiffened diaphragms and bearing adjustments. Cable forces showed reduced dynamic amplification, enhancing serviceability, though supplemental stay-specific damping devices may be required for rain-wind effects. No adverse interactions between PTMD and MTMD were identified, provided tuning bands were sufficiently separated and additional mass remained within 2-3.5% of modal masses. Sensitivity studies indicated that soil-structure interaction slightly lowered natural frequencies

but did not compromise robustness, as MTMD spread tuning preserved performance and PTMD required only minor retuning. Proper inclusion of geometric nonlinearity and cable sag was found critical, since linearized models underestimated displacements and overpredicted fragility medians by 10-18%. Finally, while wind response analyses confirmed CTMD efficiency for buffeting below flutter onset, higher-fidelity aeroelastic testing or coupled CFD-FEM modeling may refine predictions and further clarify damping interactions.

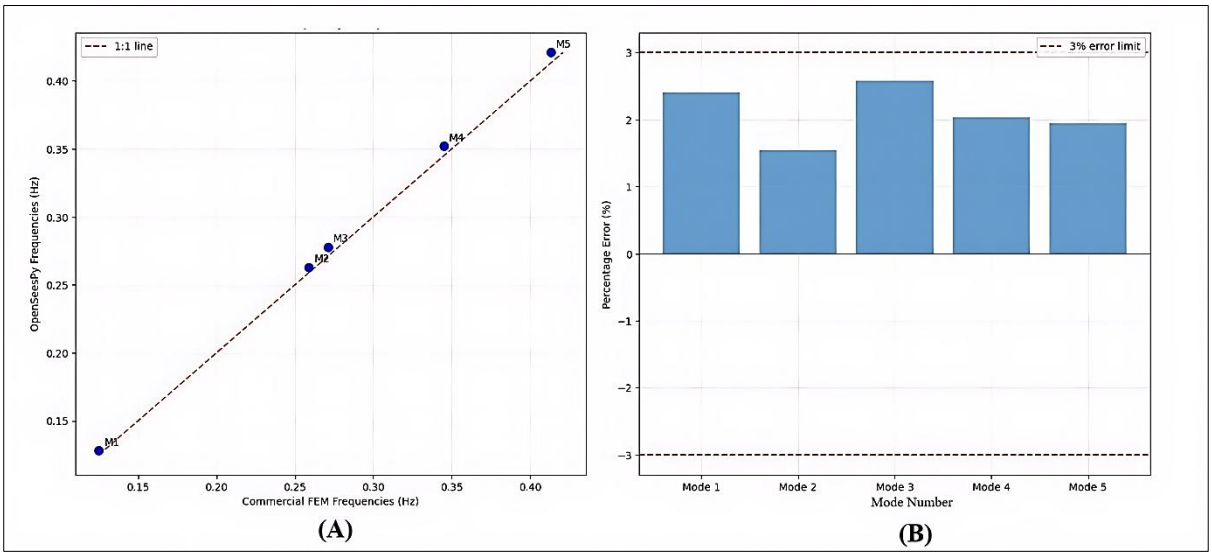

Figure 9: Numerical FEM Model Validation: (A) Modal Frequency Comparison, (B) Modal Frequency Error Distribution

For the studied 1,800 m span archetype, a pylon height of approximately 600 m offers the most balanced multi-hazard performance under the adopted seismic and wind weights, although heights in the range of 550-650 m should be evaluated for project-specific criteria. Inclusion of a tower top TMD with a mass ratio of about 1.5% is recommended for pylons of 600 m or greater to control lateral modes, with careful provision for stroke capacity and maintenance access. On the main span, an MTMD system comprising eight units distributed over the central 0.4L at 0.05L spacing and paired across the deck width provides effective control of vertical and torsional modes. A total mass ratio of about 2.0% of the generalized deck modal mass allocated across targeted modes, combined with staggered tuning of ±8% around the design frequencies and damping ratios of 12-16%, ensures robust performance even under soil-structure interaction and frequency shifts caused by temperature variation. This configuration yields reductions of 35-55% in wind-induced RMS deck response and increases of 45-75% in DS2 seismic fragility medians compared with the uncontrolled case. Detailing recommendations include strengthening diaphragms at MTMD anchorage stations, verifying bearing shear margins, and implementing monitoring systems with provisions for periodic retuning to maintain long-term control effectiveness.

Despite the comprehensive nature of the numerical framework, certain limitations should be acknowledged. The wind analysis was limited to buffeting response and did not explicitly simulate aeroelastic instabilities such as flutter or vortex-induced vibration. Bearing behavior and soil–structure interaction were idealized, and site-specific seismic hazard de-aggregation was not performed. These simplifications may influence quantitative predictions but do not alter the qualitative trends and comparative conclusions drawn from the parametric investigation.

The present study was limited to wind buffeting analysis, while aeroelastic phenomena such as flutter, vortex-induced vibration, and galloping were not simulated, indicating the need for future wind tunnel campaigns or validated CFD-based investigations to capture higher-order aerodynamic effects. Ground motion selection and scaling were based on generalized spectra, and site-specific hazard de-aggregation combined with conditional spectrum matching would provide more realistic seismic input for refined performance assessment. The archetype

configuration was idealized, and variability in cable arrangement, deck stiffness, or pylon geometry could shift the numerical optima as shown in Figure 9, warranting parametric exploration of alternative layouts. Beyond passive devices, semi-active or hybrid systems such as magnetorheological dampers or adaptive MTMDs may offer improved robustness under uncertain hazards, while integration of life-cycle cost optimization that accounts for construction, maintenance, and operational demands represents a valuable area for future research.

Conclusion

A comprehensive, reproducible computational framework was used to quantify the seismic fragility and wind buffeting performance of very long span cable stayed bridges with 500-700 m pylons and to optimize TMD deployment. For a representative 1,800 m main span bridge, an optimal pylon height near 600 m minimized a joint seismic-wind risk metric. A combined TMD strategy, one tower top TMD (μ≈1.5%) plus eight MTMD units over the central 40% of the main span (μtotal≈2.0%, s=0.05L), increased DS2 fragility medians by roughly 50-60% and cut wind RMS deck response by 40-50%, with only minor local shear increases at attachments. These findings provide actionable guidance for early design and risk screening of ultra tall cable stayed bridges. The open scripts enable replication and adaptation to site specific hazards.

Although the framework is demonstrated for cable-stayed bridges, its extension to other long-span bridge typologies is straightforward. For suspension bridges, the methodology may be adapted by targeting dominant cable and hanger modes, while for continuous girder or arch bridges, the focus may shift toward deck bending and global lateral modes. Modifications would primarily involve redefining critical engineering demand parameters and optimizing damper placement relative to the governing modal characteristics. Future research may also explore hybrid and semi-active control strategies, including magnetorheological dampers or adaptive tuned mass damper systems, to further enhance robustness under uncertain multi-hazard loading.

Abbreviations

CFRP: Carbon Fiber–Reinforced Polymer, CTMD: Combined Tuned Mass Damper (PTMD + MTMD), DS1–DS4: Damage States 1 to 4 (Slight, Moderate, Extensive, Collapse), DTMD: Deck-Mounted Tuned Mass Damper, EDP: Engineering Demand Parameter, IM: Intensity Measure, MTMD: Multiple Tuned Mass Damper, PTMD: Pylon-Top Tuned Mass Damper, P–Δ: P-delta (second-order geometric nonlinearity), RMS: Root Mean Square.

Acknowledgement

The authors gratefully acknowledge the support provided by Anjuman-I-Islam's Kalsekar Technical Campus, New Panvel, India, for facilitating the computational resources and academic environment necessary for this research.

Author Contributions

Inamdar Zakeer Ahamed Kadir Ahamed: conceptualization, methodology, software, formal analysis, investigation, data curation, visualization, writing – original draft, writing – review & editing, Rajendra B Magar: supervision, validation, resources, writing – review & editing, project administration.

Conflict of Interest

The authors declare that they have no known competing financial interests or personal relationships that could have appeared to influence the work reported in this paper.

Declaration of Artificial Intelligence (AI) Assistance

The authors confirm that no generative AI or AI-assisted technologies were used in the preparation, drafting, or editing of this manuscript. All analyses, interpretations, and writing were conducted solely by the authors. However, the authors declare that Grammarly and Zotero are used to enhance language and edit texts, do citations with a focus on grammar checks, sentence structure and citing the papers.

Ethics Approval

Not applicable. This study is based entirely on computational modeling and simulation. No human participants, animal experiments, or biological materials were involved.

Funding

This research did not receive any specific grant from funding agencies in the public, commercial, or not-for-profit sectors.

References

1. Liu J, Li H, Zhang Y, Chen G, Yang D. Stochastic seismic responses and dynamic reliability analysis of long-span cable-stayed bridge with multi-dimensional isolation and energy dissipation devices. Soil Dyn Earthq Eng. 2025;197:109560. doi:10.1016/j.soildyn.2025.109560
2. Congjie S, Huoyue X, Xiangfu T, Yulong B, Yongle L, Kou L. A design method of aeroelastic model for long-span three-tower steel truss girder cable-stayed bridges. J Wind Eng Ind Aerodyn. 2025;264:106152. doi:10.1016/j.jweia.2025.106152
3. Zhang Z, Han JY, Luo L, Zhu B, Liu YL, Cui SA, Wang XW. Experimental study on the mechanical behavior of steel in anchor systems of steel anchor boxes for long-span cable-stayed bridges. Construction and Building Materials. 2025 Jul 25;485:141918. doi:10.1016/j.conbuildmat.2025.141918
4. Qin J, Long J, Zhang M, Yuan R, Jiang F, Duan W. Long-range nighttime dynamic monitoring of long-span cable-stayed bridge with the enhanced bokeh tracking method using closing operation and long short-term memory networks. Eng Struct. 2025;342:120913. doi:10.1016/j.engstruct.2025.120913
5. Tan X, Fang Z, Chen Y, Chen J. Conceptualization and performance evaluation of a super long span cable-stayed bridge with CFRP cables and CFRP–UHPC composite girders. Case Stud Constr Mater. 2025;22:e04881. doi:10.1016/j.cscm.2025.e04881
6. Huang G, Chen C, Yan D, Zeng Y, Xu Q. Shrinkage and creep effects on long-span steel–concrete composite girder cable-stayed bridges: Modeling and structural analysis. Structures. 2025;79:109520. doi:10.1016/j.istruc.2025.109520
7. Li ZX, Zheng Q, Su J, Shi Y, Zhao B. Underwater shaking table tests of a sea-crossing cable-stayed bridge under combined earthquake and wave action. Ocean Eng. 2023;287:115871. doi:10.1016/j.oceaneng.2023.115871
8. Aloupis C, Chajes MJ, Shenton HW III. Damage identification in cable-stayed bridges based on the redistribution of dead and thermal loads. Eng Struct. 2023;284:115967. doi:10.1016/j.engstruct.2023.115967
9. Camara A, Efthymiou E. Deck–tower interaction in the transverse seismic response of cable-stayed bridges and optimum configurations. Eng Struct. 2016;124:494–506. doi:10.1016/j.engstruct.2016.06.017
10. Camara A, Astiz MA. Influence of the tower geometry on the inelastic seismic response of cable-stayed bridges. Structures. 2025;75:108752. doi:10.1016/j.istruc.2025.108752
11. Yu X, Meng X, Yu J, Chen D. Innovative design and performance analysis of steel-truss-girder cable-stayed highway bridges in mountainous regions. Structures. 2025;74:108508. doi:10.1016/j.istruc.2025.108508
12. Mazzeo M, Santoro R, Sciutteri S, Ricciardi G. Inerter-based dissipation for vibration control of a cable-stayed bridge subjected to transverse seismic excitation. Eng Struct. 2025;336:120297. doi:10.1016/j.engstruct.2025.120297
13. Li S, Wang R, Zhao Y, Zeng W, Irakoze JP. Research on the control of vortex-induced vibration of stay cable by tuned mass damper-inerter with collisions. J Sound Vib. 2025;619:119392. doi:10.1016/j.jsv.2025.119392
14. Chen D, Xie X, Lu C, Peng J, Wang L. Dynamic modeling and linear vibration characteristic of cable-stayed bridges. Part I: Theoretical modeling and variational principle. Appl Math Model. 2026;150:116375. doi:10.1016/j.apm.2025.116375
15. Li YF, He WY, Ren WX, Lu L. Main girder dynamic alignment reconstruction of cable-stayed bridge based on physics-informed neural network. Adv Eng Inform. 2025;68:103581. doi:10.1016/j.aei.2025.103581
16. Liang C, Rui Z, Zhangliang H, Wei X, Zhiming H, Yuqing H, Yingao Z. Effects of important characteristics of earthquake ground motions on probabilistic seismic demand assessment of long-span cable-stayed bridges. Structures. 2024;60:105910. doi:10.1016/j.istruc.2024.105910
17. Zhai Y, Weng G, Han Z, Zhu X, Wang B. Dynamic pressure and displacement response of pipelines in cable-stayed bridge under the coupling effect of earthquakes and crude oil flow. Results Eng. 2025;27:106719. doi:10.1016/j.rineng.2025.106719
18. Li Q, Ma C, Pei C, Chen X. Buffeting characteristics of cable-stayed box beam bridge based on pressure measurement test of full bridge aeroelastic model. Eng Struct. 2024;311:118174. doi:10.1016/j.engstruct.2024.118174
19. Jian B, Su Y, Li M. Buffeting response of cable-stayed bridge during construction under skew winds and pylon interference. KSCE J Civ Eng. 2020;24(10):2971–2979. doi:10.1007/s12205-020-1822-3
20. Zhang R, Yang B, Liu Z, Xian J, Li T, Qiao X, Chen Z. Aeroelastic system identification for predicting nonlinear unsteady coupled galloping of lamp-attached stay cables based on wind tunnel tests. Engineering Structures. 2025 Mar 15;327:119601. doi:10.1016/j.engstruct.2024.119601
21. Shen Z, Li J, Li R, Gao G. Nonuniform wind characteristics and buffeting response of a composite cable-stayed bridge in a trumpet-shaped mountain pass. J Wind Eng Ind Aerodyn. 2021;217:104730. doi:10.1016/j.jweia.2021.104730
22. Lopez-Nuñez E, Ogueta-Gutiérrez M, Gómez-Ortega O, Manzanares-Bercial R, Roibás-Millán E, Franchini S. Effect of wind barriers on the aeroelastic instabilities of a hinged-deck cross-section cable-stayed bridge. Eng Struct. 2023;287:116112. doi:10.1016/j.engstruct.2023.116112
23. Liang Y, Kong Y, Yan L, Zhao Z, Guan P. Multi-hazard fragility analysis of cross-sea cable-stayed bridges cable bent tower under seismic-wind combined action. Soil Dyn Earthq Eng. 2025;195:109422. doi:10.1016/j.soildyn.2025.109422
24. Liang Y, Zhao T, Wei Y, Guan P. Fragility analysis of cross-sea highway cable-stayed bridges under seismic-wind combined loading. Eng Fail Anal.

2025;173:109451. doi:10.1016/j.engfailanal.2025.109451
25. Yan Y, Huang H, Sun L. Multi-parameter seismic fragility and sensitivity analysis of long-span cable-stayed bridge based on multi-task lasso regression. Structures. 2022;38:1515–1528. doi:10.1016/j.istruc.2022.02.068
26. Franchini A, Sebastian W, D'Ayala D. Surrogate-based fragility analysis and probabilistic optimisation of cable-stayed bridges subject to seismic loads. Eng Struct. 2022;256:113949. doi:10.1016/j.engstruct.2022.113949
27. Maheri M, Towhata S, Okada T. Investigation of the relationship between intensity measures and engineering demand parameters of cable-stayed bridges using intra-plate earthquakes. Eng Comput. 2020;38(4):1920–1932. doi:10.1108/EC-05-2020-0255
28. Wang W, Lu C, Chen S, Chen B, Hua X. Damping enhancement of nodal modes for stay cables using a single-sided pounding tuned mass damper. Eng Struct. 2024;305:117659. doi:10.1016/j.engstruct.2024.117659
29. Peng S, Zhang L, Chen Y, Chai X. Experimental study on the performance of tuned mass damper inerter in suppressing low-frequency vibrations of long-span bridges: Model experiments and full-scale field tests. Structures. 2025;73:108357. doi:10.1016/j.istruc.2025.108357
30. Qian D, Cong Y, Kang H, Su X. Dynamics on vortex-induced vibration suppression of a flexible cable by tuned mass damper. Commun Nonlinear Sci Numer Simul. 2025;151:109129. doi:10.1016/j.cnsns.2025.109129
31. Gu M, Xiang H. Optimization of tuned mass damper for suppressing buffeting response of long-span bridges. J Wind Eng Ind Aerodyn. 1992;42(1):1383–1392. doi:10.1016/0167-6105(92)90146-2
32. Kontoni DP, Farghaly A. Mitigation of the seismic response of a cable-stayed bridge with soil–structure interaction effects using tuned mass dampers. Struct Eng Mech. 2019;69(6):699–709. doi:10.12989/sem.2019.69.6.699

How to Cite: Ahamed IZAK, Magar RB. Multi Hazard Seismic Fragility of Very Long Span Cable Stayed Bridges with Tuned Mass Dampers: Parametric Study from 500 M To 700 M Pylons and Programmatic Validation. Int Res J Multidiscip Scope. 2026; 7(1): 1779-1792. DOI: 10.47857/irjms.2026.v07i01.08307